

Demonstration of a resonance condition monitor on a silicon nanobeam cavity by using a photoconductive graphene heater

Tao Guo¹, Wei Yao², Ciyuan Qiu^{1, *}

¹Department of Electronic Engineering, Shanghai Jiao Tong University, Shanghai 200240, China

²Chongqing Institute of Green and Intelligent Technology, Chinese Academy of Sciences, Chongqing 401122, China

Author e-mail address: qiuciyuan@sjtu.edu.cn

Abstract: We demonstrate a resonance condition monitor by using a photoconductive graphene micro-heater on a silicon nanobeam cavity. The heater also shows a large thermo-optic tuning efficiency of 1.97 nm/mW to tune the resonance wavelength. © 2019 The Author(s)

OCIS codes: (130.3120) Integrated optics devices; (160.5140) Photoconductive materials

1. Introduction

Silicon-on-insulator (SOI) platform is attractive due to its compact footprint, low power consumption, and compatibility with complementary metal-oxide-semiconductor (CMOS) processes [1]. Many silicon resonant devices have been demonstrated, including micro-ring resonators (MRRs), photonic crystal nanobeams (PCNs). However, these resonance characteristics are highly sensitive to fabrication variations and fluctuations in both the chip temperature and the laser's wavelength [2]. In order to address the issue, the resonance conditions of these devices need to be monitored.

To monitor the devices' resonance conditions, several novel schemes have been demonstrated, such as on-chip photodetectors (PDs) [3] and in-resonator PDs [4]. Here, the former needs to tap light out from these devices, which might lead to the increases in device footprint and insertion losses. The latter can utilize defect state absorption (DSA) as the photodetection mechanism [4], which however would increase the complexity of fabrication processes.

Graphene, a single sheet with carbon atoms arrayed in a honeycomb structure, has received considerable interests due to its unique properties [5]. Graphene has a high thermal conductivity of up to 5,300 W/m · K [6] and a low optical loss [7], so that it can be used as a heat spreader [8], transparent heaters [9], etc. Moreover, graphene also has a strong photoconductive effect [10]. Thus, it can also be used as a high-efficient photodetector, in which its electric conductivity increases with respect to the optical intensity of illumination.

By using the abovementioned properties of graphene, in this paper, we demonstrate a resonance condition monitor by using a photoconductive graphene micro-heater covered on a silicon PCN cavity. We show that the electric conductivity of the heater would approach its maximal value at the resonance wavelength of the cavity, owing to the strong enhancement of optical intensity inside the cavity. Moreover, the heater can also be used to effectively tune the resonance wavelength with a thermo-optic (TO) efficiency of 1.97 nm/mW [11]. Thus, the photoconductive graphene heater can be used to simultaneously monitor and tune the resonance wavelength, which might find applications in the field of resonance wavelength tuning and stabilization.

2. Device design and fabrication

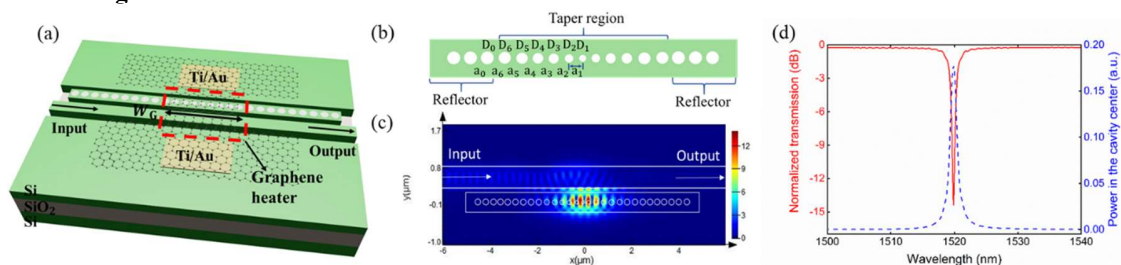


Fig. 1. (a) The 3D schematic structure of the device. The red dashed line represents the graphene heater region. (b) Top-view of the PCN cavity, which is symmetric with respect to its center. Here, D_i ($i = 0, 1, 2, 3, 4, 5, 6$) is the diameter of the hole and a_i is the center-to-center distance of adjacent holes. (c) Simulated electric field distribution of the PCN cavity at the resonance wavelength. (d) Simulated output transmission and optical intensity in the cavity as a function of the input wavelength. Here, the optical intensity is extracted at the center of the cavity.

The three-dimensional (3D) structure of the device is presented in Fig. 1(a), which consists of a bus waveguide and a

side-coupled silicon PCN cavity with a graphene sheet on top. The PCN cavity includes a central-taper region and two side-reflector regions, which can be regarded as a Fabry-Perot (F-P) cavity. The taper region has 11 holes while the reflector regions have 18 holes. As depicted in Fig. 1(b), the reflector regions with $D_0 = 225$ nm and $a_0 = 405$ nm are tapered down along six holes symmetrically around the center to $D_1 = 171$ nm and $a_1 = 307.8$ nm. The gap between the bus waveguide and the PCN waveguide is set to 77 nm. The electric field distribution of the PCN cavity is then simulated by the finite-difference time-domain (FDTD) methods. As shown in Fig. 1(c), the mode volume is only $0.198 \mu\text{m}^3$ at the resonance wavelength and the effective length for the thermal tuning is only $\sim 1.8 \mu\text{m}$. Thus, the width of covered monolayer graphene (W_G) is chosen to be $1.8 \mu\text{m}$. The optical intensity at the center of the cavity and the output power are shown in Fig. 1(d). We can find that the maximal power in the cavity center and the minimal output light power are simultaneously obtained at the resonance wavelength of the cavity. Based on the linear absorption of graphene, a maximum electric conductivity of graphene at the resonance wavelength is expected.

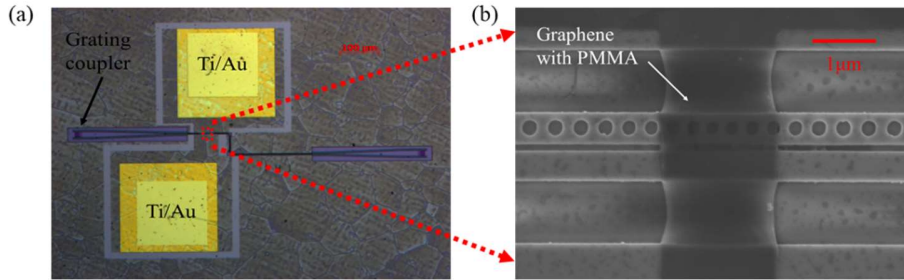


Fig. 2. (a) Microscope image of the device. (b) Zoom-in SEM image of the nanobeam waveguide with a covered graphene heater.

The device was fabricated on a SOI wafer with a 220-nm-thick top silicon layer. The device pattern was firstly defined by the standard process of electron beam lithography (EBL) and inductive coupling plasma (ICP) etching. Then, a 400-nm-thick silica layer was evaporated on the silicon layer through EBL and lift-off processes to reduce the optical losses caused by the graphene sheet. Note that, the PCN cavity was not covered by the deposited silica layer. Besides, 10 nm/100 nm Ti/Au electrodes on the silicon layer were deposited. Finally, a graphene sheet was wet-transferred onto the fabricated device and was patterned by EBL and oxygen plasma etching processes. The microscope image of the fabricated device is presented in Fig. 2(a). The zoom-in scanning electron microscope (SEM) image of the designed graphene over the PCN cavity is provided in Fig. 2(b). Here, the polymethyl methacrylate (PMMA) used for graphene pattern design was not removed, which can protect the graphene from being damaged.

3. Experimental results

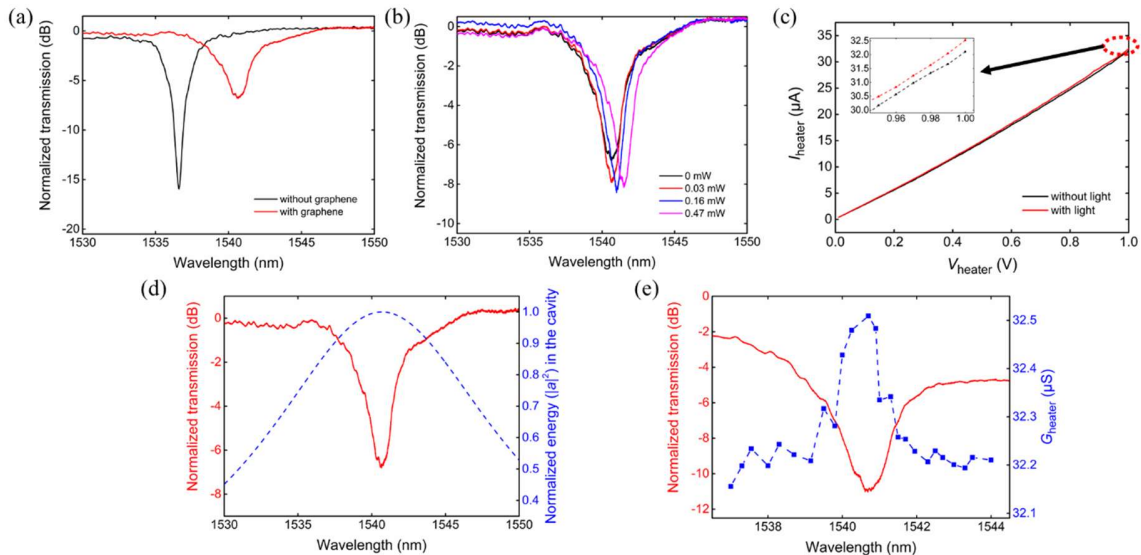


Fig. 3. (a) Normalized transmission spectra of the device without and with graphene. (b) Normalized transmission spectra of the device under different heating powers. (c) $I_{\text{heater}}-V_{\text{heater}}$ curve without (black line) and with (red line) light input; the inset shows the zoom-in results near $V_{\text{heater}} = 1$ V. (d) Measured output transmission spectrum and estimated energy ($|a|^2$) in the cavity with respect to the optical input wavelength. (e) Measured output transmission spectrum and G_{heater} as a function of the optical input wavelength when V_{heater} is 1 V.

The measured normalized transmission spectra of the device without and with graphene are depicted in Fig. 3(a). The extinction ratio (ER) of the device without graphene is ~ 16 dB. However, the ER decreases to 7 dB due to the optical loss caused by the graphene absorption. Furthermore, the total loss of the device is ~ 17 dB without graphene and ~ 19 dB with graphene. The increment in the total loss is also caused by the absorption of graphene.

The normalized transmission spectra of the device with different heating powers are provided in Fig. 3(b). When the heating power varies from 0 mW to 0.47 mW, the resonance wavelength has a red shift of ~ 0.93 nm. The estimated TO tuning efficiency is 1.97 nm/mW. One can find that, the graphene heater can effectively tune the resonance wavelength.

To demonstrate the photoconductive behavior of the heater, we characterize the current (I_{heater}) flowing through the graphene heater with respect to the voltage (V_{heater}) applied on the heater. As shown in Fig. 3(c), the black line and red line represent experimental results without and with light input, respectively. Here, the input light wavelength is fixed at 1540.7 nm, which is the resonance wavelength when V_{heater} is 1 V. The inset shows that I_{heater} increases ~ 0.42 μA with 0.45 mW light input (P_{in}) where V_{heater} is 1 V. Also, we can find that the electric conductivity (G_{heater}) of the heater increases ~ 0.42 μS where V_{heater} is 1 V. Here, G_{heater} is calculated as I_{heater} divided by V_{heater} . This increase of G_{heater} comes from the photoconductive effect of graphene as well as the enhancement of the optical power intensity inside the PCN cavity when the input light wavelength matches the resonance wavelength of the cavity. Furthermore, we define the photoconductive efficiency as the ratio of ΔG_{heater} to P_{in} . Note that, ΔG_{heater} is extracted by subtracting G_{heater} without light input from G_{heater} with light input. The graphene-heater based monitor shows a photoconductive efficiency of 0.93 mS/W in this experiment.

To show the resonance wavelength monitoring capability, we use an analytical model based on the coupled mode theory and the transfer matrix method to calculate the intrinsic quality factor (Q_i) and the coupling quality factor (Q_c). With the calculated Q_i and Q_c , the normalized energy ($|a|^2$) in the cavity can be estimated by the formulas mentioned in [12]. By putting the output transmission spectrum with the estimated normalized $|a|^2$ together in Fig. 3(d), we can find that $|a|^2$ peaks at the resonance wavelength where a minimal output power is obtained. This is consistent with the simulated results as shown in Fig. 1(d).

Due to the strong enhancement of the optical intensity at the resonance wavelength, a maximal electric conductivity could be obtained at that wavelength. Here, the measured output transmission spectrum and G_{heater} as a function of the optical input wavelength are provided in Fig. 3(e). The output light intensity decreases ~ 8 dB while G_{heater} increases ~ 0.4 μS . As expected, we can find that a maximal electric conductivity and a minimal output light intensity are obtained simultaneously at the resonance wavelength of 1540.7 nm. Thus, all the simulated, calculated and experimental results agree well with each other, which indicates that the measured electric conductivity of the graphene heater can be used to monitor the resonance condition.

4. Conclusion

We demonstrate a graphene heater with a TO tuning efficiency of up to 1.97 nm/mW, which can also be used as a resonance condition monitor on a silicon PCN cavity. Based on the experimental results, the graphene micro-heater could be used in the resonance wavelength locking where resonance wavelength monitoring and tuning are desired.

References

- [1] M. Asghari and A. V. Krishnamoorthy, "Silicon photonics: Energy-efficient communication," *Nat. Photonics* **5**, 268–270 (2011).
- [2] H. Jayatilaka, K. Murray, M. Á. Guillén-Torres, M. Caverley, R. Hu, N. A. F. Jaeger, L. Chrostowski, and S. Shekhar, "Wavelength tuning and stabilization of microring-based filters using silicon in-resonator photoconductive heaters," *Opt. Express* **23**, 25084 (2015).
- [3] J. A. Cox, A. L. Lentine, D. C. Trotter, and A. L. Starbuck, "Control of integrated micro-resonator wavelength via balanced homodyne locking," *Opt. Express* **22**, 11279 (2014).
- [4] Y. Zhang, Y. Li, S. Feng, and A. Poon, "Towards adaptively tuned silicon microring resonators for optical networks-on-chip applications," *IEEE J. Sel. Topics Quantum Electron.* **20**, 136–149 (2014).
- [5] A. K. Geim and K. S. Novoselov, "The rise of graphene," *Nat. Mater.* **6**, 183–191 (2007).
- [6] A. A. Balandin, S. Ghosh, W. Bao, I. Calizo, D. Teweldebrhan, F. Miao, and C. N. Lau, "Superior thermal conductivity of single-layer graphene," *Nano Lett.* **8**, 902–907 (2008).
- [7] M. Liu, X. Yin, E. Ulin-Avila, B. Geng, T. Zentgraf, L. Ju, F. Wang, and X. Zhang, "A graphene-based broadband optical modulator," *Nature* **474**, 64–67 (2011).
- [8] R. Prasher, "Graphene spreads the heat," *Science* **328**, 185–186 (2010).
- [9] L. Yu, Y. Yin, Y. Shi, D. Dai, and S. He, "Thermally tunable silicon photonic microdisk resonator with transparent graphene nanoheaters," *Optica* **3**, 159 (2016).
- [10] X. Sun, C. Qiu, J. Wu, H. Zhou, T. Pan, J. Mao, X. Yin, R. Liu, W. Gao, Z. Fang, and Y. Su, "Broadband photodetection in a microfiber-graphene device," *Opt. Express* **23**, 25209 (2015).
- [11] Z. Xu, C. Qiu, Y. Yang, Q. Zhu, X. Jiang, Y. Zhang, W. Gao, and Y. Su, "Ultra-compact tunable silicon nanobeam cavity with an energy-efficient graphene micro-heater," *Opt. Express* **25**, 19479 (2017).
- [12] T. Pan, C. Qiu, J. Wu, X. Jiang, B. Liu, Y. Yang, H. Zhou, R. Soref, and Y. Su, "Analysis of an electro-optic modulator based on a graphene-silicon hybrid 1D photonic crystal nanobeam cavity," *Opt. Express* **23**, 23357 (2015).